

Stable optical trapping of latex nanoparticles with ultrashort pulsed illumination

Arijit Kumar De,¹ Debjit Roy,¹ Aavek Dutta,² and Debabrata Goswami^{1,2,*}

¹Department of Chemistry, Indian Institute of Technology, Kanpur UP-208016, India

²Laser Technology Program, Indian Institute of Technology, Kanpur UP-208016, India

*Corresponding author: dgoswami@iitk.ac.in

Received 16 April 2009; revised 24 June 2009; accepted 6 July 2009;
posted 6 July 2009 (Doc. ID 110151); published 22 July 2009

Here we report how ultrafast pulsed illumination at low average power results in a stable three-dimensional (3D) optical trap holding latex nanoparticles which is otherwise not possible with continuous wave lasers at the same power level. The gigantic peak power of a femtosecond pulse exerts a huge instantaneous gradient force that has been predicted theoretically earlier and implemented for microsecond pulses in a different context by others. In addition, the resulting two-photon fluorescence allows direct observation of trapping events by providing intrinsic 3D resolution. © 2009 Optical Society of America

OCIS codes: 350.4855, 300.2530.

1. Introduction

Optical waveguides have illuminating applications in numerous experiments that spatially deliver electromagnetic waves at optical wavelengths. One such example is the optical tweezer or single beam gradient optical trap that makes use of a tightly focused laser beam having a transverse Gaussian intensity profile to trap particles of various sizes ranging from a few micrometers to a few nanometers. Over the past few decades laser tweezers have grown from a mere trapping instrument to a powerful tool to measure and control tiny forces that dictate many fundamental physical, chemical, and biological processes. Detailed discussions on various aspects of optical trapping can be found in numerous reviews [1–3] and texts [4,5]. The major advantage of laser tweezers over mechanical transducers, e.g., scanning force microscopy (SFM), cantilevers, or microneedles, is the accessible low force range (from 10^{-10} to 10^{-13} N) that they offer, which renders them more suitable for biological applications [6].

Recently, there have been several reports to trap and manipulate individual metallic and dielectric nanoparticles by laser tweezers instead of traditional methods such as atomic force microscopy (AFM). These are of utmost importance in manipulating and patterning nanoparticles to achieve different needs, e.g., spectroscopy of trapped particles based on localized surface plasmon (LSP) [7] and Raman measurement [8], nanolithography [9], trapping and manipulating carbon nanotubes [10], and gold nanoparticles [11]. Even viruses and bacteria, ranging in size from a few tens to a few hundred nanometers, have been trapped optically [12]. All these experiments suffered from their own drawbacks. The experiments made use of cw near-infrared (NIR) lasers to trap particles with diameters (d) nearly an order of magnitude smaller than the laser wavelength ($\lambda \sim 800\text{--}1100$ nm); therefore the trapping forces are largely governed by Rayleigh scattering where the particle is regarded as a point dipole. For Rayleigh particles in the limit of $1/k \gg d$ ($k = 2\pi/\lambda$ being the wavenumber), the gradient force (F) on the dipolar particle equals [13]

$$F = \left(\frac{\alpha}{2}\right) \nabla E^2,$$

where E is the optical electric field and α is the polarizability given by

$$\alpha = \left(\frac{n^2 - 1}{n^2 + 2} \right) r^3,$$

with n being the refractive index and r the radius of the trapped particle. This shows the need for an objective with a high numerical aperture (NA) required to maximize ∇E^2 so that the transverse gradient force takes over the axial scattering force resulting in a stable trap. Also, since the polarizability depends on the volume, in the dipole limit smaller particles are more difficult to trap than larger ones. The minimum laser power needed to trap single-walled carbon nanotubes [10] or tobacco-mosaic viruses (TMVs) [12] has been found to be 100 mW. It is interesting to note here that, although the volume of these particles satisfy the Rayleigh criterion, the actual dimensions do not; e.g., in one experiment [12] the cylindrical TMV had a length of 320 nm, which is close to the trapping wavelength (514.5 nm) used. A spherical particle is an automatic choice to avoid this issue. However, earlier efforts [14] revealed that higher power levels are required to stably trap latex nanoparticles; the exertable force was found to be smaller for latex nanoparticles than for gold nanoparticles, making the former a poor choice for nanoscale applications. Another problem is direct observation of trapped nanoparticles under traditional white light illumination (bright-field microscopy) methods for observing trapping of Mie particles ($\lambda \gg d$). Alternative choices of using other far-field observation methods such as differential interference contrast (DIC)[11] or fluorescence [10] microscopic techniques suffer from the fact that the maximum resolution is bound by the diffraction limit that is much more than the particle diameter. In addition, the presence of scattering or luminescent background obscures the image, which can be taken care of by confocal detection for fluorescence-based methods. Also, observation by scattering of auxiliary laser light [15] acts as perturbation to the trapping laser field.

We have shown how ultrafast pulses lead to stable trapping of latex nanoparticles three dimensionally in space at power levels where cw lasers cannot lead to a stable trap. In addition, background-free two-photon fluorescence from the trapped particles provides a unique way of observing them, which is much better than the scattering-based methods.

2. Experiment

The experimental setup sketched in Fig. 1 is a thoroughly modified version of our previous arrangement as described elsewhere [16]. We used NIR (centered at 780 nm) ~ 120 fs mode-locked pulsed excitation (at 76 MHz pulse repetition rate) of a Ti:sapphire laser (Mira900-F pumped by Verdi5, Coherent Incorporated) that can also operate in a cw mode. Two-photon fluorescence was induced when the laser

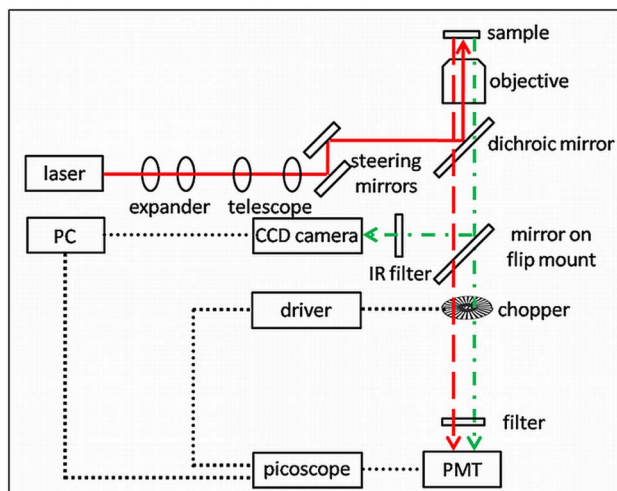


Fig. 1. (Color online) Experimental setup. The excitation beam path is shown as a solid (red) line, while the backscattered path is shown as a dashed (red) line. The fluorescence collection path is shown as a dashed-dot (green) line.

was operated in the pulsed mode. The expanded laser beam, shown as a solid (red) line, was passed through a telescopic arrangement along with two steering mirrors and sent to the microscope objective (UPLSAPO 1.4 NA 100XO, Olympus Incorporated) of a completely homemade benchtop inverted microscope. A dichroic mirror, placed just before the objective lens, has $\sim 95\%$ reflectance at 780 nm; at the same wavelength the objective transmits $\sim 65\%$ yielding $\sim 60\%$ of the light at the sample. This was confirmed by measuring the laser power with a powermeter (FieldMate, Coherent) as well as a silicon amplified photodiode (PDA100A-EC, Thorlabs). The two-photon-induced fluorescence, shown as a dashed-dot (green) line, as well as the backscattered light, shown as a dashed (red) line, was collected by a photomultiplier tube (PMT) using appropriate band-pass filters. The PMT signal was collected by an automotive oscilloscope or picoscope (Pico Technology) triggered by a rotating-disk optical chopper (with a 30 slot wheel) run by a tunable frequency driver (MC1000A, Thorlabs) and operating at 800 Hz. Thus, our robust setup is capable of measuring the two-photon fluorescence as well as the backscattered light to observe trapping of tiny nanoparticles in real time; it can also acquire video microscopy by bright-field illumination (not shown) and dark-field fluorescence generation. We trapped fluorophore (having single-photon absorption maxima at 540 nm and an emission maximum at 560 nm) coated polystyrene 100 nm diameter latex beads (F8800, Molecular Probes). A dilute and slightly alkaline (pH of ~ 8) solution of the sample was well sonicated and was used immediately for the trapping experiments to avoid aggregation. The 780 nm pulsed excitation simultaneously traps as well as generates backscattered (under both pulsed and cw modes) as well as fluorescence signals (only under a pulsed mode). Since in this case the wavelength of trapping light

is nearly eight times larger than the particle diameter, the particle dimensions are in the Rayleigh regime.

3. Results and Discussion

The laser was first set to operate in a pulsed mode. At ~ 10 mW the time-averaged laser power at the sample tweezing is evident by occurrence of random spikes into the trapping zone [17] with seldom seen trapping that lasted a few seconds [see Fig. 2(b)]. The height of the signal directly corresponds to the number of particles being trapped simultaneously. A more stable trap was observed when the average power was elevated to 30 mW as shown in Figs. 3(a) and 3(b) depicting fluorescence and a backscattered signal, respectively. Figure 3(a) clearly shows trapping of a single particle followed by another one; the relative strength of fluorescence has nearly a 1:2 ratio (after background subtraction), which confirms the number of trapped particles (the spikes with larger heights are due to aggregates rapidly diffusing across the

focal volume). However, when the laser was switched to the cw mode, the tweezing action had much higher power (~ 100 mW), and a stable trap with subsequent particle aggregation was observed at an even higher power (~ 200 mW) as shown in Fig. 4. Thus, these results clearly indicate the crucial role of ultrashort pulses in trapping tiny particles as explained below.

Multiphoton fluorescence has been previously combined with optical trapping using cw excitation [18,19]. The main advantage of nonlinear fluorescence generation is that, since it is confined only within the tiny focal volume [20,21], any persistent fluorescence signal corresponds only to the trapped particles that can be observed despite the presence of many other out-of-focus particles within the cone of illumination. Also, the effect of two-photon absorption on force calibration is negligible; since the probability of two-photon absorption is very low, we can completely neglect recoil force that is due to absorption of photons arriving in one direction with omnidirectional emission [5]. This is one advantage over using auxiliary lasers for observation by scattering

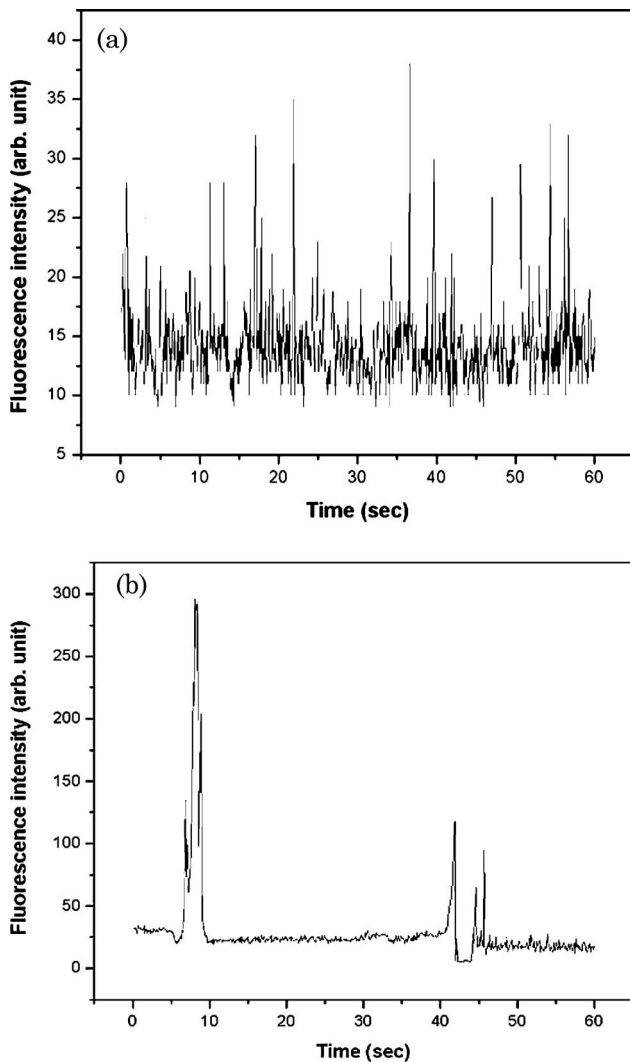


Fig. 2. Fluorescence signal at 10 mW laser power: (a) frequent spikes showing biased diffusion and (b) trapping for a few seconds.

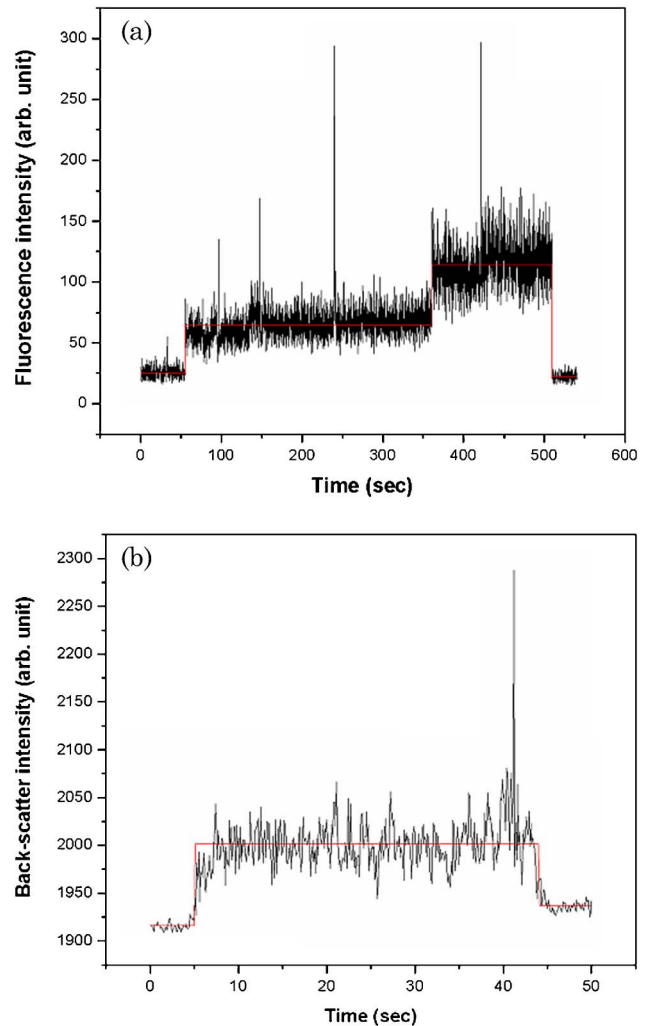


Fig. 3. (Color online) (a) Fluorescence and (b) backscattered signals (black curves) along with their step-function fits (red curves) at 30 mW laser power.

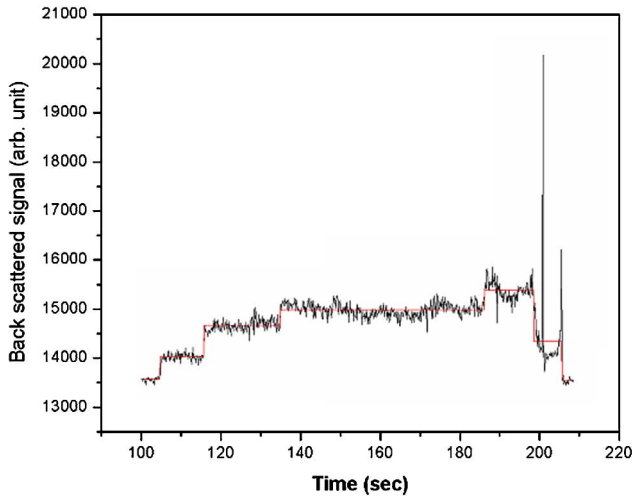


Fig. 4. (Color online) Backscattered signal (black curve) along with the step-function fit (red curve) for cw excitation at 200 mW.

as the secondary laser light perturbs the trapping force field.

The use of cw lasers for multiphoton absorption has been surpassed by mode-locked subpicosecond pulsed lasers to circumvent the low absorption cross sections of common fluorophores. Owing to its fleeting temporal existence, a femtosecond laser pulse has enormous peak power compared with its time averaged power; the typical ratio between them being $10^5:1$. The high photon flux increases the trap stiffness (or force constant) to such an extent that a stable trap is observed at the same average power level of cw lasers that cannot trap nanoparticles. Wang and Zhao [22] derived an analytical expression for instantaneous longitudinal and transverse (gradient) radiation force components for pulsed excitation acting on Rayleigh particles; each pulse exerts a ponderomotive force on the particle, and the steepness of the associated potential well overcomes the Brownian fluctuations leading to a stable trap. The calculations have shown that the necessary condition for trapping is given by the Boltzmann factor, $\exp(-U_{\max}/k_B T)$, with

$$U_{\max} = \pi \epsilon_0 n_1^2 r^3 \left| \frac{m^2 - 1}{m^2 + 2} \right| \times \frac{4 \sqrt{2} U}{n_2 \epsilon_0 c \omega^2 \pi^{3/2} \tau},$$

where k_B is the Boltzmann constant; T is the absolute temperature; ϵ_0 is the vacuum permittivity; n_1 and n_2 are the refractive indices of the particle and surroundings, respectively, with $m = n_1/n_2$; r is the radius of the trapped particle; U is the pulse energy; c is the speed of light in vacuum; ω_0 is the beam radius at the focus (taken to be $\sim 1 \mu\text{m}$); and τ is the pulse width. At 20°C and 780nm , n_1 and n_2 are 1.57845 and 1.32896, respectively (www.refractive-index.info). For 30mW average power, U is nearly 0.3 nJ , yielding the Boltzmann factor to be $\ll 1$, indicating that radiation force can overcome thermal motions. Our finding is also supported by the previously reported use of short pulses ($\sim 45 \mu\text{s}$ duration)

capable of overcoming adhesive interaction between a glass surface and the particles attached to the glass due to large peak gradient force ($\sim 10^{-9}\text{ N}$) [23].

For a Mie particle Brownian motion is sluggish and a shallow potential well (offered by a cw or time-averaged pulsed laser) is good enough to trap it. In contrast, a rapidly moving Rayleigh particle cannot be trapped with a shallow force field, but it can be efficiently trapped when the well depth is steep, provided the particle does not diffuse away within the time period of the periodic force field (discussed in detail in the following section). In other words, to realize the effects of instantaneous forces, we must design an experiment that can sense the difference between cw versus pulsed excitation, and trapping Rayleigh particles is one such experiment as the random Brownian motion of a tiny Rayleigh particle is sensitive to the instantaneous force field. This is precisely the reason why the stiffness of an ultrashort laser trap has been reported to be equal to that with cw excitation with the same average power [19]. Even earlier theoretical calculations [24] failed to differentiate between cw and pulsed excitation due to sampling of the pulses. As we discussed above, the Wang and Zhao theory [22] managed to distinctively provide evidence of stable trapping with femtosecond laser pulses, which is distinctly evident in our experiments. However, experimental measurement of the instantaneous force by a femtosecond pulse is not possible by any of the present-day techniques for measuring trap stiffness; for example, the time scales associated with the viscous drag method are so slow compared with the pulse rate that the instantaneous force averages out. Therefore, further research needs to be pursued with regard to the precise measurement of instantaneous trap stiffness.

The pulse repetition rate is a crucial factor for stably trapping Rayleigh particles. Within $\sim 13\text{ ns}$ (inverse of 76 MHz) the time lag between two consecutive pulses and the already trapped particle does not leave the trapping region. Considering Brownian motion of the 100 nm particle, let us assume that the particle moves in a straight line in a single step during the blanking time of the laser such that, during that time interval, it covers the maximum path distance. For a Brownian particle, the distance covered after a single step is given by

$$l = \sqrt{2D\tau},$$

where D is the diffusion coefficient of the 100 nm polystyrene beads in water and is given by

$$D = \frac{k_B T}{6\pi\eta r},$$

where η is the viscosity coefficient. At the experimental condition of 20°C , D is $\sim 5 \times 10^{-12}\text{ m}^2\text{s}^{-1}$, which gives the value of l to be $\sim 0.36\text{ nm}$ which is very much smaller than the dimensions of the focal volume (having a nearly diffraction-limited dimension

of $\sim 1 \mu\text{m}$); hence the particle cannot leave the focal volume when the trapping light is off. This is also in complete agreement with theoretical predictions by Wang and Zhao [22]. Now the size of the particle dictates whether it will leave a trap within the time period when no light is present to hold it. Thus for a fixed focal dimension there is an optimal trade-off between the particle diameter and the pulse repetition rate for the particle being trapped over time. The high repetition-rate (HRR) lasers seem to be a good choice for this reason. The additional advantage of using pulsed lasers is that it causes minimal heating compared with cw excitation [25] owing to possible heat diffusion during the interpulse time lag. Also, since the two-photon-induced heating is largely mediated by solvent [26], the low absorption coefficient of water at the NIR wavelength used [27] makes it suitable for biological applications.

4. Conclusion

In summary, we have shown how to exploit the huge pulse power of ultrafast pulsed lasers with a high repetition rate to hold tiny Rayleigh particles that were thought to be untrappable at low optical power levels. In addition, the method offers clear observation of trapping events owing to the nonlinear fluorescence generation. However, much work is still needed to calibrate the instantaneous stiffness that is due to a single pulse. Trapping and manipulating particles of much smaller size by use of this technique are currently being pursued in our laboratory.

A. K. De and D. Roy thank the Council of Scientific and Industrial Research (CSIR), India, for graduate fellowships. We also thank the Department of Science and Technology (DST), India, and the Wellcome Trust Foundation, UK, for funding. The help from Saptaparna Das, Shaon Chakrabarty, and Anirban Roy is gratefully acknowledged.

References

1. A. Ashkin, "Applications of laser radiation pressure," *Science* **210**, 1081–1088 (1980).
2. A. Ashkin, "History of optical trapping and manipulation of small-neutral particle, atoms and molecules," *IEEE J. Sel. Top. Quantum Electron.* **6**, 841–855 (2000).
3. K. C. Neuman and S. M. Block, "Optical trapping," *Rev. Sci. Instrum.* **75**, 2787–2809 (2004).
4. P. M. Sheetz, ed., *Laser Tweezers in Cell Biology* (Academic, 1998).
5. A. Ashkin, *Optical Trapping and Manipulation of Neutral Particles Using Lasers: a Reprint Volume with Commentaries* (World Scientific, 2006).
6. C. Bustamante, J. C. Macosko, and G. J. L. Wuite, "Grabbing the cat by the tail: manipulating molecules one by one," *Nat. Rev. Mol. Cell Biol.* **1**, 130–136 (2000).

7. J. Prikulis, F. Svedberg, M. Käll, J. Enger, K. Ramser, M. Goksör, and D. Hanstorp, "Optical spectroscopy of single trapped metal nanoparticles in solution," *Nano Lett.* **4**, 115–118 (2004).
8. K. Ajito and K. Torimistu, "Single nanoparticle trapping using a Raman tweezers microscope," *Appl. Spectrosc.* **56**, 541–544 (2002).
9. D. L. J. Vossen, D. Fific, J. Penninkhof, T. van Dillen, A. Pollman, and A. van Blaaderen, "Combined optical tweezers/ion beam technique to tune colloidal masks for nanolithography," *Nano Lett.* **5**, 1175–1179 (2005).
10. S. Tan, H. A. Lopez, C. W. Cai, and Y. Zhang, "Optical trapping of single-walled carbon nanotubes," *Nano Lett.* **4**, 1415–1419 (2004).
11. P. M. Hansen, V. K. Bhatia, N. Harrit, and L. Oddershede, "Expanding the optical trapping range of gold nanoparticles," *Nano Lett.* **5**, 1937–1942 (2005).
12. A. Ashkin and J. M. Dziedzic, "Trapping and manipulation of viruses and bacteria," *Science* **235**, 1517–1520 (1987).
13. P. A. M. Neto and H. M. Nussenzweig, "Theory of optical tweezers," *Europhys. Lett.* **50**, 702–708 (2000).
14. K. Svoboda and S. M. Block, "Optical trapping of metallic Rayleigh particles," *Opt. Lett.* **19**, 930–932 (1994).
15. J. Zhou, L. Qu, K. Yao, M. Zhong, and Y. Li, "Observing nanometre scale particles with light scattering for manipulation using optical tweezers," *Chin. Phys. Lett.* **25**, 3995 (2008).
16. A. K. De, D. Roy, B. Saha, and D. Goswami, "A simple method for constructing and calibrating an optical tweezer," *Curr. Sci.* **95**, 723–724 (2008).
17. D. T. Chiu and R. N. Zare, "Biased diffusion, optical trapping, and manipulation of single molecules in solution," *J. Am. Chem. Soc.* **118**, 6512–6513 (1996).
18. Y. Liu, G. J. Sonek, M. W. Berns, K. Konig, and B. J. Tromberg, "Two-photon fluorescence excitation in continuous-wave infrared optical tweezers," *Opt. Lett.* **20**, 2246–2248 (1995).
19. B. Agate, C. T. A. Brown, W. Sibbert, and K. Dholakia, "Femtosecond optical tweezers for in-situ control of two-photon fluorescence," *Opt. Express* **12**, 3011–3017 (2004).
20. W. Denk, J. H. Strickler, and W. W. Webb, "Two-photon laser scanning fluorescence microscopy," *Science* **248**, 73–76 (1990).
21. S. Maiti, J. B. Shear, R. M. Williams, W. R. Zipfel, and W. W. Webb, "Measuring serotonin distribution in live cells with three-photon excitation," *Science* **275**, 530–532 (1997).
22. L. Wang and C. Zhao, "Dynamic radiation force of a pulsed Gaussian beam acting on a Rayleigh dielectric sphere," *Opt. Express* **15**, 10615–10621 (2007).
23. A. A. Ambarekar and Y. Li, "Optical levitation and manipulation of stuck particles with pulsed optical tweezers," *Opt. Lett.* **30**, 1797–1799 (2005).
24. Q. Xing, F. Mao, L. Chai, and Q. Wang, "Numerical modeling and theoretical analysis of femtosecond laser tweezers," *Opt. Laser Technol.* **36**, 635–639 (2004).
25. E. J. G. Peterman, F. Gittes, and C. F. Schmidt, "Laser-induced heating in optical traps," *Biophys. J.* **84**, 1308–1316 (2003).
26. A. K. De and D. Goswami, "Exploring the nature of photo-damage in two-photon excitation by fluorescence intensity modulation," *J. Fluoresc.* **19**, 381–386 (2009).
27. G. M. Hale and M. R. Querry, "Optical constants of water in the 200 nm to 200 μm wavelength region," *Appl. Opt.* **12**, 555–563 (1973).